



LJMU Research Online

Leitao, RCF, Trujillo, LN, Leitao, A and Albuquerque, RQ

On the use of porous nanomaterials to photoinactivate E. coli with natural sunlight irradiation

<http://researchonline.ljmu.ac.uk/id/eprint/4164/>

Article

Citation (please note it is advisable to refer to the publisher's version if you intend to cite from this work)

Leitao, RCF, Trujillo, LN, Leitao, A and Albuquerque, RQ (2015) On the use of porous nanomaterials to photoinactivate E. coli with natural sunlight irradiation. Solar Energy, 122. pp. 1117-1122. ISSN 0038-092X

LJMU has developed **LJMU Research Online** for users to access the research output of the University more effectively. Copyright © and Moral Rights for the papers on this site are retained by the individual authors and/or other copyright owners. Users may download and/or print one copy of any article(s) in LJMU Research Online to facilitate their private study or for non-commercial research. You may not engage in further distribution of the material or use it for any profit-making activities or any commercial gain.

The version presented here may differ from the published version or from the version of the record. Please see the repository URL above for details on accessing the published version and note that access may require a subscription.

For more information please contact researchonline@ljmu.ac.uk

<http://researchonline.ljmu.ac.uk/>

On the use of porous nanomaterials to photoinactivate *E. coli* with natural sunlight irradiation

Renan C. F. Leitao, Loren N. Trujillo, Andrei Leitao^{*}, Rodrigo Q. Albuquerque^{*}

São Carlos Institute of Chemistry, University of São Paulo, 13560-970 São Carlos, Brazil

^{*} Corresponding author

E-mail: rodrigo_albuquerque@iqsc.usp.br; Phone: +55 (16) 3373-8779

E-mail: andleitao@iqsc.usp.br; Phone: +55 (16) 3373-9943

Abstract

An organic-inorganic hybrid material based on nanocrystals of zeolite L functionalized with silicon phthalocyanine can develop interesting properties when activated by natural sunlight. Cell viability tests show that this nanomaterial is able to photoinactivate mouse cells and *Escherichia coli* (*E. coli*) bacteria, and is also very efficient against the self-defense mechanisms of *E. coli* during the first minutes of solar irradiation. The results suggest that Gram-negative *E. coli* become more resistant to singlet oxygen-based disinfection treatments at higher temperatures. The present work contributes to the development of new functional materials for a range of important sunlight-based applications.

Keywords: Zeolite L. Phtalocyanine. *Escherichia coli*. Photoinactivation. Natural sunlight.

1. Introduction

Each day a huge quantity of solar energy reaches our planet, which vastly exceeds the human's yearly power consumption (Lewis, 2007). From the many uses sunlight may have, solving water disinfection problems may become one of its most noble applications. Large incidence of mortality can be seen worldwide caused by polluted water and children are the most affected with many deaths everyday (Blanco et al., 2009). Additionally, the presence of pathogens in irrigation water not only damages crops, but also is responsible for the widespread use of hazardous chemicals in crop fields (Rodriguez-Mozaz et al., 2015). The combination of sunlight and appropriate photoactive materials may be used to tackle this problem (Sun et al., 2013; Schüler et al., 2013).

In sunny countries, solar water disinfection seems to be a very interesting alternative to help improve water quality [Nalwanga, et al., 2014]. Solar water disinfection using a compound parabolic collector has

reported to efficiently inactivate *Salmonella sp.* and *E. coli* [Sciacca, et al., 2010]. Ergaieg *et al* (2008) have reported the photoinactivation of Gram-positive and Gram-negative *E. coli* using porphyrin derivatives and have also discussed the different mechanisms (Types I and II) involved in the phototoxicity of their photosensitizer. Other methods for water decontamination use natural or artificial solar irradiation and TiO₂ nanoparticles to promote the photodegradation of different chemicals (Schüler, et al., 2013; Vilela et al., 2012; Rengifo-Herrera et al., 2010). Some applications involving photoinactivation of pathogens using artificial light have been made using different materials, where the cytotoxic singlet oxygen (¹O₂) is often generated (Chauhan et al., 2013; Ballatore et al., 2015; Rengifo-Herrera et al., 2010). In these treatments, ¹O₂ is produced via energy transfer from the triplet state of the excited photosensitizer to the ground triplet state of oxygen (³O₂). Ru(II) photosensitizers have been reported to efficiently photoinactivate *E. coli* and *Enterococcus faecalis* also via ¹O₂ generation after sunlight exposure (Jiménez-Hernández, et al., 2006).

Phthalocyanines (PCs) are often used as photosensitizers, since they present high quantum yields for the generation of triplet state (Ishii, 2012), efficiently generating ¹O₂. Numerous studies have investigated the generation of ¹O₂ by PC excitation not only in photodynamic treatments (Ding et al., 2015; Vankayala et al., 2013; Long et al., 2013; Pasparakis, 2013) but also in degradation of organic pollutants in water (Xiong et al., 2005; Sun et al., 2010; Zanjanchi et al., 2010). PCs have large planar conjugated π systems, which are responsible for the main drawback associated to this class of compounds: they easily aggregate strongly reducing their ability to generate ¹O₂ upon irradiation (Grüner et al., 2013). One elegant solution to this problem is the functionalization of PC onto high-specific surface area materials like nanoparticles or nanocrystals, which leads to novel functional hybrid materials (Choi et al., 2012; Mthethwa et al., 2015).

Zeolites can also be used to build PC-based hybrid materials for ¹O₂ generation. This was the case of zeolite L functionalized with PC, which has been reported by one of the authors to generate ¹O₂, as well as to photoinactivate pathogens via a Type I mechanism upon irradiation of artificial light (Strassert et al., 2009). Zeolite L is composed of SiO₄ and AlO₄ tetrahedral units and synthetic crystals with different shapes can be obtained in the size range of 30 to 40000 nm (Kehr et al., 2010). The symmetry of the crystals is hexagonal and the stoichiometry of each unit cell is (M₉)[Al₉Si₂₇O₇₂].nH₂O, where M is a monovalent cation, *e.g.* K⁺, and *n* = 21 for fully hydrated crystals (Calzaferri et al., 2003). The advantage

of using zeolite L over other materials lies in its parallel one-dimensional nanochannels, where energy transfer between encapsulated dyes can be easily controlled, as reported by Lutkouskaya and Calzaferri (2006), therefore offering interesting possibilities to add up new functionalities to the hybrid material. The combination between Zeolite L and phthalocyanines has been explored by Lopez-Duarte et al. (2011) to design new antenna materials.

In this work we have used a hybrid material composed of nanocrystals of zeolite L functionalized with Silicon 2,9,16,23-tetra-*tert*-butyl-29H,31H-phthalocyanine dihydroxide (SiPC) to promote the photoinactivation of different living organisms (mouse cells and *E. coli*) using natural sunlight.

2. Experimental section

2.1 Sample preparation

The zeolite L crystals (ca 50 nm long) were obtained from the Clariant GmbH company. SiPC was purchased from Sigma-Aldrich and functionalized onto the surface of zeolite L nanocrystals (nZeol) after refluxing a suspension of the crystals in chlorobenzene to produce nZeol-SiPC. The presence of bulky *tert*-butyl groups is important to reduce the SiPC aggregation, which increases its solubility in chlorobenzene. The surface of the crystals was further functionalized with 3-aminopropyltriethoxysilane (APTES) to improve the adherence of the nanomaterial to the negatively charged cell wall, as zeta potential measurements have already shown that these particles are positively charged at pH 7.4 (Strassert et al., 2012). The prepared nanomaterial is abbreviated as nZeol-SiPC/APTES. More details about the synthesis of the nanomaterial are available in the SI.

2.2 Viability assays for BALB/c.

As a pilot test to evaluate the nanomaterial efficiency to photoinactivate biological systems using natural sunlight, cell viability tests were first conducted using penicillin/streptomycin-resistant mouse BALB/c 3T3 clone A31 cells, which are mammalian cells widely used for cytotoxicity studies. Cell viability experiments were performed in closed quartz cuvettes (4.5 cm x 1 cm x 1 cm, 3.5 mL). For all experiments containing the nanomaterial, 1 mg of nZeol-SiPC/APTES was suspended in 1.5 mL of PBS, and 0.5 mL of cell suspension (in PBS) was added to that mixture. Negative control experiments were carried out using: i) cells + nanomaterial in the dark; ii) cells in the dark; iii) cells + sunlight. Samples

were exposed to natural sunlight irradiation under continuous stirring. The sunlight irradiance (1000 Wm^{-2}) was measured using a solar power meter and all experiments were done in the city of São Carlos, Brazil (Latitude $22^{\circ} 01' 04''$ South; Longitude $47^{\circ} 53' 27''$ West). Sampling was performed by collecting 0.1 mL of the reaction mixture in a 96-well plate at time intervals of 0, 30, 60 and 90 min of irradiation. The cells were analyzed on a Merck-Millipore guava easyCyte 8HT flow cytometer using the Guava ViaCount software module after sample incubation during at least 5 min with ViaCount® reagent in the dark. For comparison purposes, viability experiments were also carried out with artificial white light (ca 300 Wm^{-2} of irradiance) using a Tungsten lamp.

2.3 Viability assays for *E. Coli* bacteria

Cell counting of *E. coli* was performed with the ViaCount® reagent following the procedure of the manufacturer. Due to the high number of cells, dilutions were performed to achieve 4×10^7 cells mL^{-1} . The cell death was determined after irradiating 2 ml of a PBS suspension containing *E. coli* (1×10^7 cells mL^{-1}) and nZeol-SiPC/APTES (1 mg) with natural sunlight. This system was then kept under sunlight exposure and 0.1 mL was collected every 30 minutes. The same negative control experiments carried out for BALB/c cells were also done here (vide supra). For the cell death quantification a dilution was made to reduce the cell concentration to 5×10^5 cells mL^{-1} , thereafter 50 μL of cells were mixed with 200 μL of ViaCount® reagent following at least 5 min of incubation. The viability profile and cell counting of *E. coli* in all systems tested were analyzed on a Merck-Millipore guava easyCyte 8HT flow cytometer using the guava InCyte 2.7 software. Two independent experiments were performed in triplicate. The cultivation procedures of both cells (BALB/c and *E. coli*) are available in the Supporting Information (SI). The local temperature during all experiments was about 30°C . It was observed that the size of the nanozeolites was interfering with the *E. coli* readout. This was caused by the tendency of positively-charged zeolites to aggregate when in contact with the negatively-charged membrane of *E. coli* cells. This problem was dealt with by changing the sensitivity of the equipment and gating the samples based on cells without any treatment.

3. Results and discussion

The excitation and emission spectra of nZeol-SiPC suspended in CH_2Cl_2 peaks at 679 nm and 684 nm, respectively (Fig. 1a), which is characteristic of SiPC in the monomeric form, since SiPC aggregates are

not luminescent. The diffuse reflectance spectrum of nZeol-SiPC in powder showed the characteristic Q-band of SiPC with maximum absorption at 682 nm. This band is broader and slightly red-shifted when compared with the one observed in the absorption spectrum of SiPC in CH_2Cl_2 ($\lambda_{\text{max}} = 679 \text{ nm}$, Fig. S1). This result may be due to the interaction between SiPC and the zeolite crystals in the nanomaterial, as well as due to the strong interactions usually observed in solid-state systems. Nanozeolite L crystals functionalized with SiPC were also characterized by thermogravimetric analysis (Fig. 1b), from which we have estimated 10^4 SiPC molecules per zeolite crystal, which indicates a high coverage of the crystals.

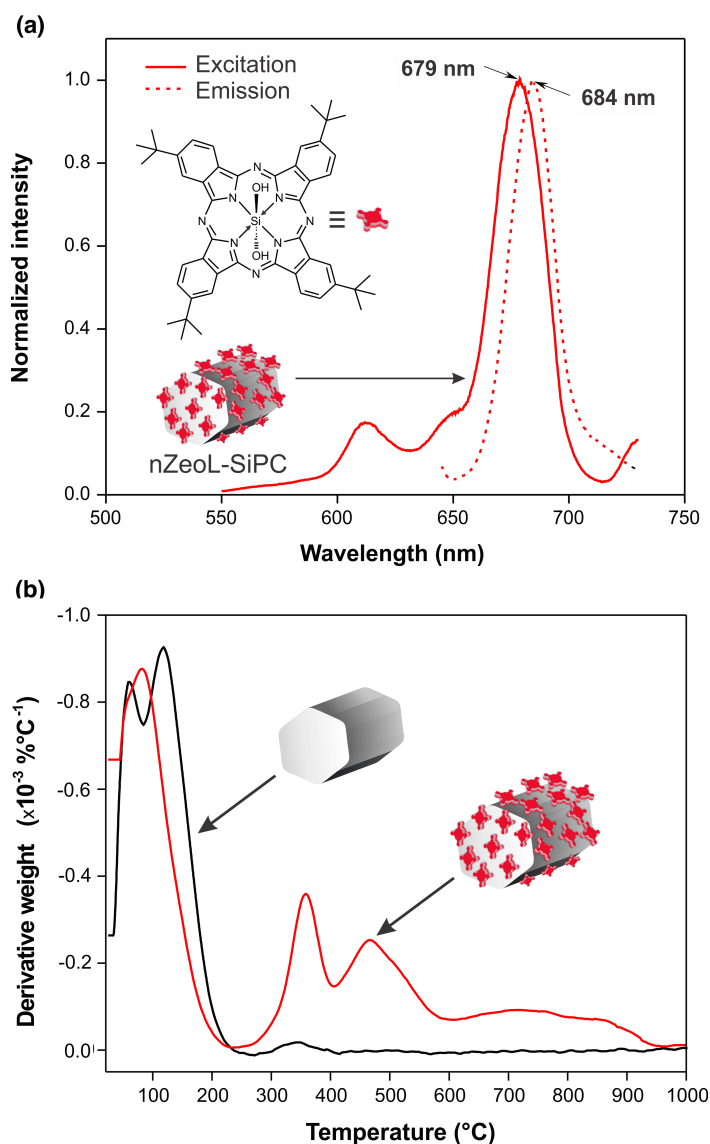


Fig. 1. (a) Excitation and emission spectra of nZeol-SiPC suspended in CH_2Cl_2 at room temperature ($\lambda_{\text{exc}}/\lambda_{\text{em}} = 640/730 \text{ nm}$) and (b) derivative thermogravimetric analysis (DTG) of nZeol (black line) and nZeol-SiPC (red line).

It has been reported that the PC-zeolite Si-O-Si binding in such system occurs via the attachment of the axial OH group of PC to one of the Si-OH groups of the zeolite surface (Grüner et al., 2013). The ninhydrin test was used to confirm the presence of amino groups on the crystals. The presence of APTES on nZeol-SiPC/APTES is revealed by a strong purple color formed after the reaction of the amino groups with ninhydrin. The characteristic absorption bands of the product formed (Ruhemann's purple) were observed at 400 and 570 nm (Fig. S2), confirming the existence of amino groups on the crystals' surface.

Cell viability tests were initially conducted using penicillin/streptomycin-resistant mouse BALB/c 3T3 clone A31 cells as a pilot test to evaluate the efficiency of our nanomaterial. The number of surviving cells (cell viability) after different periods of time was determined through flow cytometry experiments using a fluorophore that intercalates into the DNA of non-viable cells. The BALB/c assays (Fig. 2(a)) show a large quantity of photoinactivated cells in the presence of nZeol-SiPC/APTES under natural sunlight exposure (1000 Wm^{-2}). Less than 9 % of the cells were still viable within 30 minutes of irradiation in the presence of nZeol-SiPC (red bars).

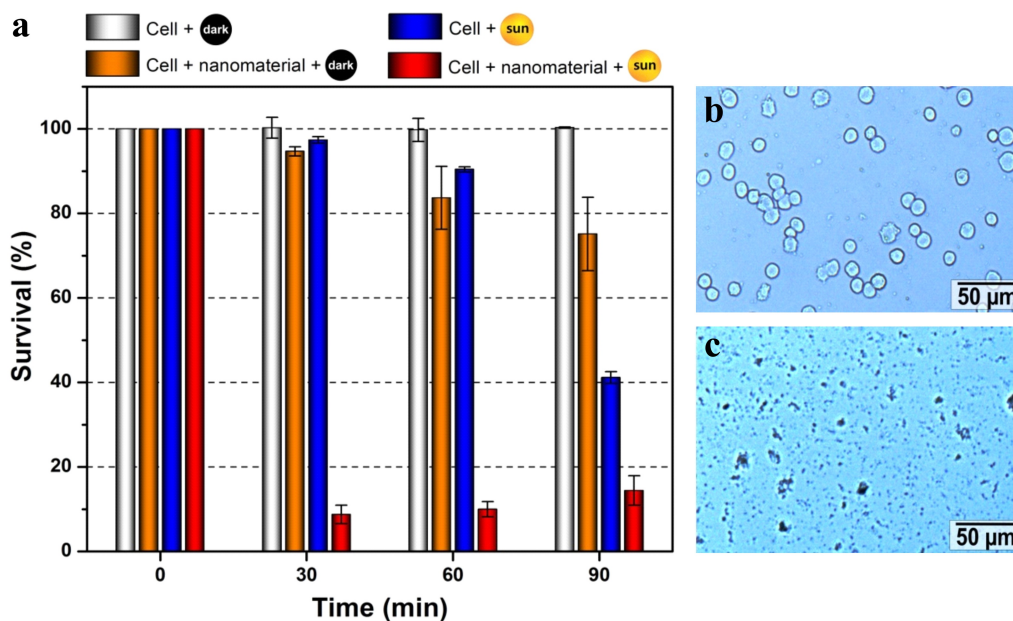


Fig. 2. (a) Cell viability assays using BALB/c cells suspended in PBS under different conditions. Microscopy images at 10X of BALB/c cells before (b) and after (c) 30 min irradiation in the presence of nZeol-SiPC/APTES (c). Experiments were done in triplicate in two different days.

For the same period of time, the cell viability measured in control experiments was much higher: 95 % (cells and nanomaterial in the dark, orange bars), 97 % (only sunlight irradiation, blue bars), and 100 % (cells in the dark, grey bars). This clearly shows that the mouse cells are photoinactivated by the combination of sunlight and nZeol-SiPC/APTES. Microscopy images of BALB/c cells before and after 30 min treatment are shown in Figs. 2(b) and (c), revealing the damages caused by the nanomaterial in the cells upon natural sunlight irradiation.

We carried out additional viability tests using a Xenon lamp (300 Wm^{-2}) as the light source. nZeol-SiPC/APTES has also damaged the BALB/c cells to a large extent, although, in contrast to the sunlight assays, more time was necessary to achieve the same percentage of non-viable cells (Fig. S3). This is consistent with the lower intensity of the artificial light when compared with sunlight. Differences in shape between the power spectrum of white light and sunlight may also have contributed to the different photoinactivation efficiencies, but this minor effect was not investigated here.

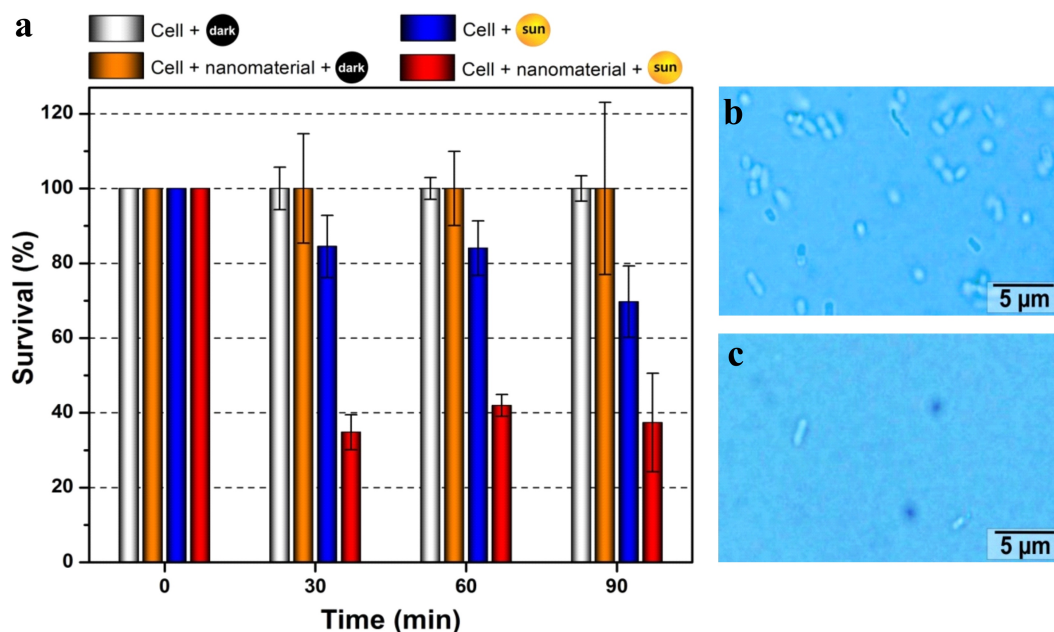


Fig. 3. (a) Cell viability assays using *E. coli* cells suspended in PBS under different conditions. Microscopy images at 100X of *E. coli* cells before (b) and after (c) 90 min sunlight irradiation in the presence of nZeol-SiPC/APTES. Experiments were done in triplicate in two different days.

Cell viability assays using Gram-negative *E. coli* bacteria were then carried out to further test the prepared nanomaterial. The same protocol as described for BALB/c cells was adopted. The

combination of nZeol-SiPC/APTES and sunlight irradiation has also lead to photoinactivation of *E. coli* cells, as pointed out in Fig. 3(a). Again, the combination of nanomaterial and sunlight was responsible for the highest photoinactivation efficiency. Figs. 3 (b) and (c) show microscopy pictures of *E. coli* before and after 90 min of sunlight irradiation in the presence of nZeol-SiPC/APTES. The images clearly show a decrease in the number of intact bacteria after the treatment.

Similarly to the pilot study carried out with BALB/c cells, cellular death was also observed when *E. coli* cells were exposed to sunlight in the absence of the nanomaterial. This is consistent with the fact that sunlight irradiation can inhibit DNA replication and also induce bacterial mutations. However, it is also known that cellular death induced only by sunlight can be slow in the first minutes of exposure due to two different self-defense mechanisms of these cells, as reported by Rincón and Pulgarin (2003). Fig. 4 shows a much faster photoinactivation of *E. coli* induced by nZeol-SiPC/APTES and natural sunlight within the first 30 min, when compared with the bacteria death after exposure to the same irradiation in the absence of nanomaterial. This reveals our nanomaterial is very efficient against the self-defense mechanisms.

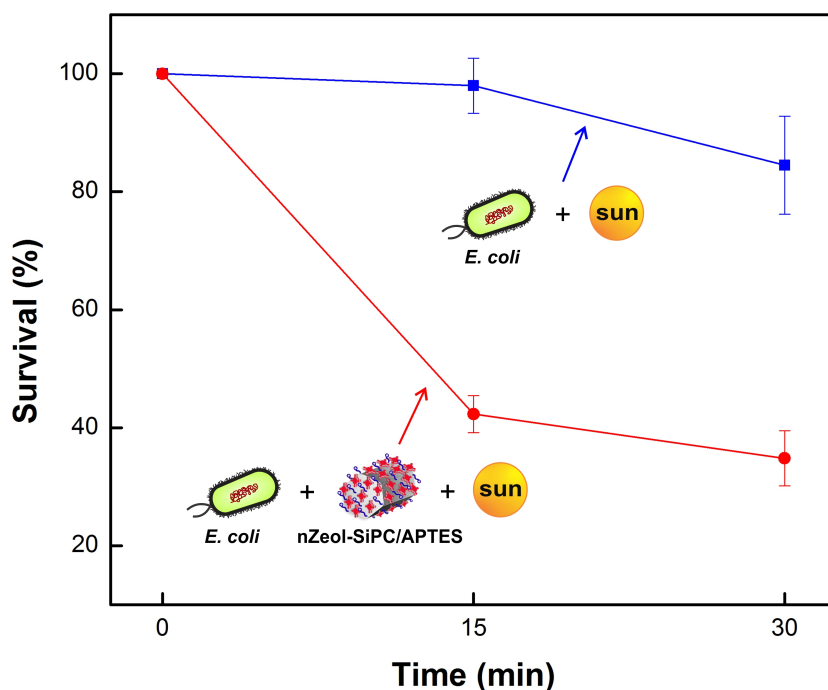


Fig. 4. Influence of the nanomaterial on the viability of *E. coli* cells in the first minutes of sunlight irradiation (1000 Wm^{-2}). Experiments were done in triplicate in two different days.

At longer exposure times the efficiency of our nanomaterial towards photoinactivation of *E. coli* using natural sunlight was not so large as one would have expected. Another photoinactivation experiment reported by one of the authors (Strassert, et al., 2009) carried out for a similar system but using much less intense artificial red light has shown considerably higher photoinactivation efficiencies at longer exposure times. The key point to understand this contrast seems to be the temperature used during the experiments, which was about 30 °C for the present work and 22 °C for the other one. It has been reported by Rincón and Pulgarin (2003) that temperature can influence the efficiency of a photocatalytic disinfection in two different and opposite ways: while Gram-positive bacteria become less resistant to that treatment upon increasing the temperature from 23 to 45 °C, Gram-negative bacteria become more resistant to such photocatalytic treatment *upon heating*. This can explain why the final disinfection efficiency of our experiments carried out at 30 °C for Gram-negative *E. coli* was not so high. This also indicates that the temperature trend reported by Rincón and Pulgarin (2003) is not only valid for photocatalytic disinfection experiments, but also for our photoinactivation experiments, which are primarily based on singlet oxygen generation. These results suggest that sunlight-based photodynamic treatment of pathogens using singlet oxygen-based methods may be more appropriate to photoinactivate Gram-positive bacteria, provided the treatment is carried out in Brazil, where local temperatures are considerably high over the whole year.

Conclusion

The present investigation has proved that natural sunlight and nZeol-SiPC-APTES can be successfully combined to photoinactivate mouse cells and pathogens in water. The developed nanomaterial was very efficient against the self-defense mechanisms of *E. coli* during the first minutes of natural sunlight irradiation. The comparison between this work and another one reported by one of the authors indicates that Gram-negative *E. coli* become more resistant to singlet oxygen-based disinfection treatments at higher temperatures. Disinfection treatments based on singlet oxygen generation and carried out in Brazil, where temperatures are relatively high over the whole year, may be more appropriate to photoinactivate Gram-positive pathogens. Finally, this work contributes to the development of new functional materials for a range of important sunlight-based disinfection applications. We are currently investigating how energy transfer inside the zeolite channels can enhance the efficiency of our photodynamic treatment.

Acknowledgments

This work was supported by the Brazilian agencies FAPESP (grants 2012/02955-5 and 2013/18009-4) and CNPq (grant 305082/2013-2). The authors acknowledge the Clariant GmbH company for providing the nanocrystals of zeolite L and Thaisa Matos for the thermogravimetric analysis.

References

- Ballatore, M. B., Durantini, J., Gsponer, N. S., Suarez, M. B., Gervaldo, M., Otero, L., Spesia, M. B., Milanesio, M. E., Durantini, E. N., 2015. Photodynamic inactivation of bacteria using novel electrogenerated porphyrin-fullerene C60 polymeric films. *Environ. Sci. Technol.* 49, 7456–7463.
- Blanco, J., Malato, S., Fernández-Ibañez, P., Alarcón, D., Gernjak, W., Maldonado, M. I., 2009. Review of feasible solar energy applications to water processes. *Renew. Sust. Energ. Rev.* 13, 1437-1445.
- Calzaferri, G., Huber, S., Maas, H., Minkowski, C., 2003. Host–Guest Antenna Materials. *Angew. Chem. Int. Ed.* 42, 3732-3758.
- Chauhan, P., Hadad, C., Sartorelli, A., Zarattini, M., Herreros-López, A., Mba, M., Maggini, M., Prato, M., Carofiglio, T., 2013. Nanocrystalline cellulose–porphyrin hybrids: synthesis, supramolecular properties, and singlet-oxygen production. *Chem. Commun.* 49, 8525-8527.
- Choi, K.-H., Lee, H.-J., Park, B. J., Wang, K.-K., Shin, E. P., Park, J.-C., Kim, Y. K., Oh, M.-K., Kim, Y.-R., 2012. Photosensitizer and vancomycin-conjugated novel multifunctional magnetic particles as photoinactivation agents for selective killing of pathogenic bacteria. *Chem. Commun.* 48, 4591-4593.
- Ding, X., Han, B.-H., 2015. Copper phthalocyanine-based CMPs with various internal structures and functionalities. *Chem. Commun.* 51, 12783-12786.
- Ergaieg, K., Chevanne, M., Cillard, J., Seux, R., 2008. Involvement of both Type I and Type II mechanisms in Gram-positive and Gram-negative bacteria photosensitization by a meso-substituted cationic porphyrin. *Solar Energy*, 82, 1107-1117.
- Grüner, M., Siozios, V., Hagenhoff, B., Breitenstein, D., Strassert, C. A., 2013. Structural and Photosensitizing Features of Phthalocyanine-Zeolite Hybrid Nanomaterials. *Photochem. Photobiol.* 89, 1406-1412.
- Ishii, K., 2012. Functional singlet oxygen generators based on phthalocyanines. *Coord. Chem. Rev.* 256, 1556-1568.
- Jiménez-Hernández, M. E., Manjón, F., García-Fresnadillo, D., Orellana, G., 2006. Solar water disinfection by singlet oxygen photogenerated with polymer-supported Ru(II) sensitizers. *Solar Energy*, 80, 1382-1387.
- Kehr, N.S., Riehemann, K., El-Gindi, J., Schäfer, A., Fuchs, H., Galla, H.J., De Cola, L., 2010. Cell Adhesion and Cellular Patterning on a Self-Assembled Monolayer of Zeolite L Crystals. *Adv. Funct. Mater.* 20, 2248-2254.
- Lewis, N. S., 2007. Toward cost-effective solar energy use. *Science* 315, 798-801.

- Long, R., Mao, K., Ye, X., Yan, W., Huang, Y., Wang, J., Fu, Y., Wang, X., Wu, X., Xie, Y., Xiong, Y., 2013. Surface facet of palladium nanocrystals: A key parameter to the activation of molecular oxygen for organic catalysis and cancer treatment. *J. Am. Chem. Soc.* 135, 3200-3207.
- Lopez-Duarte, I., Dieu, L.-Q., Dolamic, I., Martinez-Diaz, M.V., Torres, T., Calzaferri, G., Bruhwiler, D., 2011. On the Significance of the Anchoring Group in the Design of Antenna Materials Based on Phthalocyanine Stopcocks and Zeolite L. *Chem. Eur. J.* 17, 1855-1862.
- Lutkouskaya, K., Calzaferri, G., 2006. Transfer of Electronic Excitation Energy between Randomly Mixed Dye Molecules in the Channels of Zeolite L. *J. Phys. Chem. B* 110, 5633-5638.
- Mthethwa, T., Nyokong, T., 2015. Photoinactivation of *Candida albicans* and *Escherichia coli* using aluminium phthalocyanine on gold nanoparticles. *Photochem. Photobiol. Sci.* 14, 1346-1356.
- Nalwanga, R., Quilty, B., Muyanja, C., Fernandez-Ibañez, P., McGuigan, K. G., 2014. Evaluation of solar disinfection of *E. coli* under Sub-Saharan field conditions using a 25L borosilicate glass batch reactor fitted with a compound parabolic collector. *Solar Energy* 100, 195-202.
- Pasparakis, G., 2013. Light-induced generation of singlet oxygen by naked gold nanoparticles and its implications to cancer cell phototherapy. *Small* 9, 4130-4134.
- Rengifo-Herrera, J. A., Pulgarin, C., 2010. Photocatalytic activity of N, S co-doped and N-doped commercial anatase TiO₂ powders towards phenol oxidation and *E. coli* inactivation under simulated solar light irradiation. *Solar Energy* 84, 37-43.
- Rincón, A.G., Pulgarin, C., 2003. Photocatalytical inactivation of *E. coli*: effect of (continuous–intermittent) light intensity and of (suspended–fixed) TiO₂ concentration. *Appl. Catal. B: Environ.* 44, 263-284.
- Rodriguez-Mozaz, S., Ricart, M., Köck-Schulmeyer, M., Guasch, H., Bonnineau, C., Proia, L., De Alda, M. L., Sabater, S., Barceló, D., 2015. Pharmaceuticals and pesticides in reclaimed water: efficiency assessment of a microfiltration–reverse osmosis (MF–RO) pilot plant. *J. Hazard. Mater.* 282, 165-173.
- Schüler, E., Gustavsson, A.-K., Hertenberger, S., Sattler, K., 2013. Solar photocatalytic and electrokinetic studies of TiO₂/Ag nanoparticle suspensions. *Solar Energy* 96, 220-226.
- Sciacca, F., Rengifo-Herrera^c, J. A., Wéthé, J., Pulgarin, C., 2011. Solar disinfection of wild *Salmonella sp.* in natural water with a 18 L CPC photoreactor: Detrimental effect of non-sterile storage of treated water. *Solar Energy* 85, 1399-1408.
- Strassert, C. A., Otter, M., Albuquerque, R. Q., Höne, A., Vida, Y., Maier, B., De Cola, L., 2009. Photoactive Hybrid Nanomaterial for Targeting, Labeling, and Killing Antibiotic-Resistant Bacteria. *Angew. Chem. Int. Ed.* 48, 7928-7931.
- Sun, B., Qiao, Z., Shang, K., Fan, H., Ai, S., 2013. Facile synthesis of silver sulfide/bismuth sulfide nanocomposites for photocatalytic inactivation of *Escherichia coli* under solar light irradiation. *Mater. Lett.* 91, 142-145.
- Sun, Q., Xu, Y., 2010. Sensitization of TiO₂ with aluminum phthalocyanine: factors influencing the efficiency for chlorophenol degradation in water under visible light. *J. Phys. Chem. C* 113, 12387-12394.

- Vankayala, R., Kuo, C.-L., Sagadevan, A., Chen, P.-H., Chiang, C.-S., Hwang, K. C., 2013. Morphology dependent photosensitization and formation of singlet oxygen ($^1\Delta_g$) by gold and silver nanoparticles and its application in cancer treatment. *J. Mater. Chem. B* 1, 4379-4387.
- Vilela, W. F. D., Minillo, A., Rocha, O., Vieira, E. M., Azevedo, E. B., 2012. Degradation of [D-Leu]-Microcystin-LR by solar heterogeneous photocatalysis (TiO_2). *Solar Energy*, 86, 2746-2752.
- Xiong, Z., Xu, Y., Zhu, L., Zhao, J., 2005. Photosensitized oxidation of substituted phenols on aluminum phthalocyanine-intercalated organoclay. *Environ. Sci. Technol.* 39, 651-657.
- Zanjanchi, M. A., Ebrahimian, A., Arvand, M., 2010. Sulphonated cobalt phthalocyanine-MCM-41: an active photocatalyst for degradation of 2,4-dichlorophenol. *J. Hazard Mater.* 175, 992-1000.

On the use of porous nanomaterials to photoinactivate *E. coli* with natural sunlight irradiation

Renan C. F. Leitao^a, Loren N. Trujillo^a, Andrei Leitao^{*a} and Rodrigo Q. Albuquerque^{*a}

^a São Carlos Institute of Chemistry (IQSC), University of São Paulo, 13560-970 São Carlos, Brazil;

Supplementary Information

INDEX

	Page
1. Materials	13
2. General experimental procedures	14
2.1. Functionalization of Zeolite L	14
2.2. Cell culture for BALB/c	14
2.3. Cell culture for <i>E. coli</i> bacteria	14
2.4. Ninhydrin test	14
3. Characterization	15
Fig. S1. Diffuse reflectance of the prepared materials	15
Fig. S2. Colorimetric ninhydrin test	16
Fig. S3. Cell viability assays of BALB/c	17
4. References	17

1. Materials

Nano-sized zeolite L Lucidot® crystals were obtained from Clariant GmbH (primary particles size 30-60 nm). Silicon 2,9,16,23-tetra-*tert*-butyl-29*H*,31*H*-phthalocyanine dihydroxide (Dye content 80%), Chlorobenzene (anhydrous, 99.8%), Chlorobenzene (ACS reagent, ≥99.5%), Dichloromethane (anhydrous, ≥99.8%), Toluene (ACS reagent), 3-Aminopropyltriethoxysilane (≥98%), Genapol® X-080 and Lysogeny broth (LB) culture medium were obtained from Sigma-Aldrich. Ninhydrin (p.a. ACS reagent, 99%) and Triethylamine (99%) were purchased from Vetec, Brazil. Dulbecco's Modified Eagle's Medium (DMEM), Trypsin/EDTA solution, Fetal Bovine Serum (FBS) and phosphate buffer solution (PBS) were obtained from Cultilab, Brazil. Mouse fibroblast cell (BALB/C 3T3) clone A31 was acquired from the Brazilian Cell Bank (BCRJ code: 0047). *Escherichia coli* cells (CBMAI 0696) were purchased from the Multidisciplinary Chemical, Biological and Agricultural Research Center (CPQBA), Brazil. Penicillin/streptomycin solution was obtained from Vitrocell. Sodium bicarbonate and Glucose was acquired from AMRESCO and Guava ViaCount® Reagent for Flow Cytometry from Merck-Millipore.

2. General Experimental Procedures

2.1. Functionalization of Zeolite L

Zeolite L nanocrystals were first dried for 24 h in a muffle furnace at 200°C. 300 mg of dry nanocrystals and 50 mL of anhydrous chlorobenzene were transferred to a Teflon vessel and sonicated for 30 min in order to reduce the nanocrystal aggregation. Subsequently, 60 mg of phthalocyanine (SiPC) were added and N₂ was bubbled for 10 min to remove moisture from the system. After 30 min of ultrasonic bath the system was refluxed at 135°C for 6 h under stirring. The functionalized zeolite nanomaterial (nZeol-SiPC) was collected by centrifugation (15 min at 14,000 rpm). The recovered material was washed sequentially with chlorobenzene, toluene, dichloromethane, 0.2% surfactant Genapol® solution and deionized water for removing non-covalently bonded SiPC. Finally, 3-Aminopropyltriethoxysilane (APTES) functionalization on zeolite surface (nZeol-SiPC/APTES) was performed following a method reported in literature (Kallury, et al., 1994).

2.2. Cell culture for BALB/c

Cells were grown in an incubator with 5% CO₂ at 37°C and 90% humidity in DMEM supplemented with 3.5 g L⁻¹ glucose solution, 10% FBS and 1% penicillin/streptomycin solution. Cell suspension was made using 0.25% trypsin/EDTA solution (incubated for 10 min), followed by the addition of 20% FBS in PBS (pH 7.4). The suspension was centrifuged (5 min at 1,000 rpm) and the supernatant was removed. The cell concentration was determined using a Neubauer counting chamber by re-suspending the supernatant in 1 mL of culture medium. The final BALB/c cell concentration used for the experiments cited below was 10⁶ cells mL⁻¹.

2.3. Cell culture for *E. coli* bacteria

The *E. coli* cells were cultured at room temperature in LB medium. Passage of cells was performed the day before the analysis, following overnight incubation and the subsequent flow cytometry data processing.

2.4. Ninhydrin test

The presence of APTES functionalized on the zeolite surface was confirmed qualitatively by the ninhydrin reaction. Initially, the ninhydrin test solution was prepared by dissolving 0.5 g of ninhydrin reagent in 40 mL of 1-butanol and 10 mL of deionized water (Huber and Calzaferri, 2004). Then, 10 mg of nZeol-SiPC/APTES were added in 3 mL of ninhydrin test solution and stirred for 30 min at room temperature. The suspension obtained was centrifuged and photographic images were obtained to observe the color change of the ninhydrin solution after the ninhydrin reaction. The same ninhydrin test was carried out with free APTES. Finally, UV-Vis absorption of both resulting solutions was performed and their absorbances compared (See fig. S2).

3. Characterization

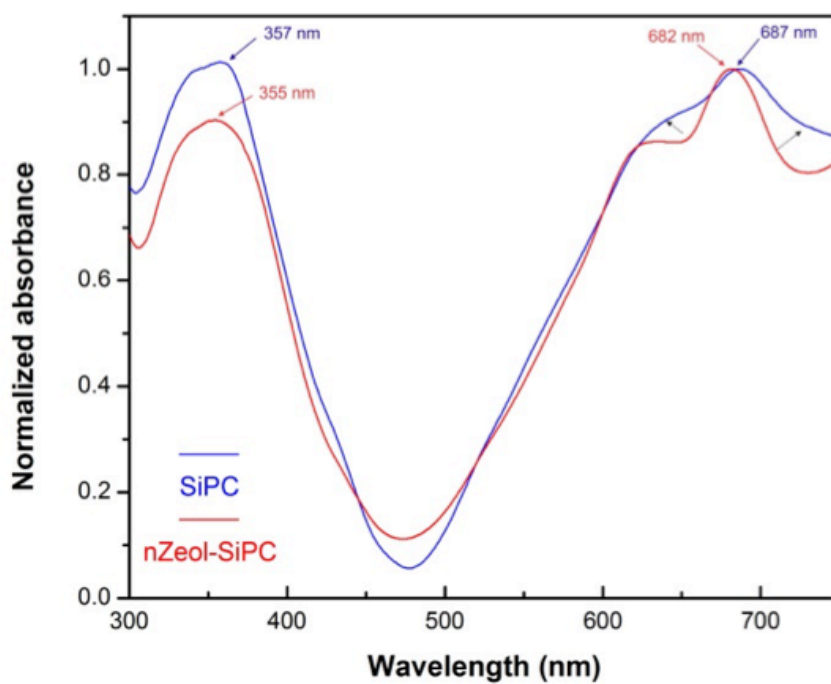


Fig. S1 Diffuse reflectance of solid SiPC (blue) and solid nZeol-SiPC (red line).

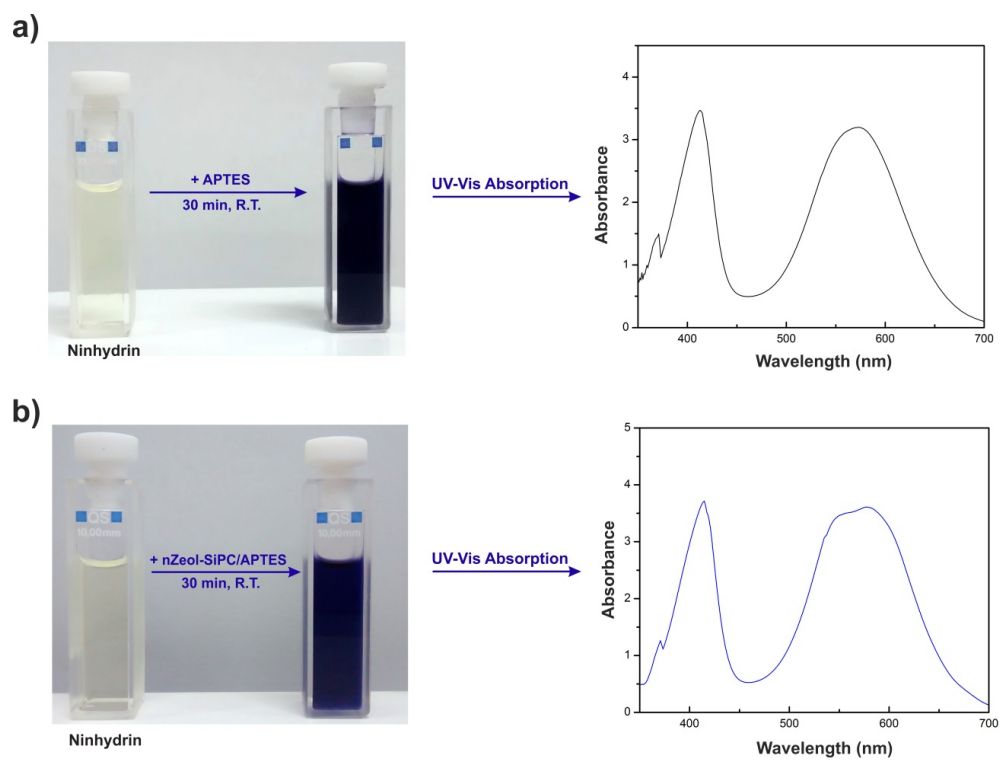


Fig. S2 Colorimetric ninhydrin test. Absorption spectra after reaction of (a) free APTES; 0.5 μL in 3 mL of ninhydrin solution and (b) nZeol-SiPC/APTES; 10 mg of nanomaterial in 3 mL of ninhydrin solution.

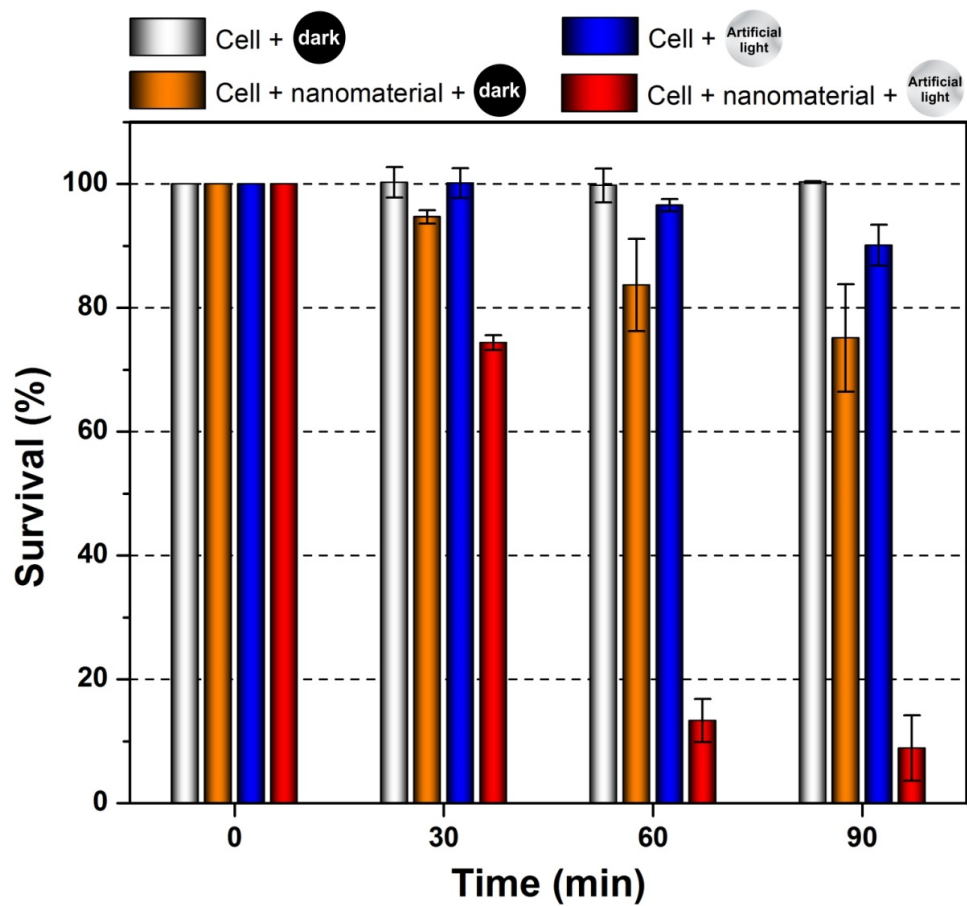


Fig. S3. Cell viability assays of BALB/c cells suspended in PBS under artificial light irradiation (Tungsten lamp, 300 Wm^{-2}) with and without nanomaterial (nZeol-SiPC/APTES) and the respective dark control assays. Experiments were done in triplicate in two different days.

4. References

- Huber, S. and Calzaferri, G., 2004. Sequential Functionalization of the Channel Entrances of Zeolite L Crystals. *Angew. Chem. Int. Ed.*, 43, 6738-6742.
- Kallury, K. M. R., Macdonald, P. M. and Thompson, M., 1994. Effect of Surface Water and Base Catalysis on the Silanization of Silica by Aminopropylalkoxysilanes Studied by X-ray Photoelectron Spectroscopy and ^{13}C Cross Polarization/Magic Angle Spinning Nuclear Magnetic Resonance. *Langmuir* 10, 492-499.